ARTICLE

Growth, ROS Markers, Antioxidant Enzymes, Osmotic Regulators and Metabolic Changes in Tartary Buckwheat Subjected to Short Drought

Yan Wan[1,#], Yuan Liang[1,#], Xuxiao Gong[1,#], Jianyong Ouyang[1], Jingwei Huang[2], Xiaoyong Wu[1], Qi Wu[1], Changying Liu[1], Xueling Ye[1], Xiaoning Cao[3], Gang Zhao[1], Liang Zou[1,*] and Dabing Xiang[1,*]

[1]Key Laboratory of Coarse Cereal Processing, Ministry of Agriculture and Rural Affairs, Sichuan Engineering & Technology Research Center of Coarse Cereal Industrialization, College of Food and Biological Engineering, Chengdu University, Chengdu, 610106, China

[2]School of Preclinical Medicine, Chengdu University, Chengdu, 610106, China

[3]Center for Agricultural Genetic Resources Research, Shanxi Agricultural University, Taiyuan, 030031, China

*Corresponding Authors: Dabing Xiang. Email: xiangdabing@cdu.edu.cn; Liang Zou. Email: zouliang@cdu.edu.cn

#This author contributed equally to this work

ABSTRACT

Tartary buckwheat (*Fagopyrum tataricum*) is an important pseudocereal feed crop with medicinal and nutritional value. Drought is one of the main causes of reduced growth and yield in these plants. We investigated the growth, physiological, and metabolic responses of the widely promoted Tartary buckwheat variety Chuan Qiao No. 1 to polyethylene glycol (PEG)-mediated drought stress. Drought significantly decreased shoot length, shoot biomass and relative water content. Root length, malondialdehyde content, electrolyte leakage, activities of superoxide dismutase, peroxidase, catalase and amylase, and contents of soluble sugar, soluble protein and proline were increased by PEG-mediated drought. Untargeted metabolomics analysis identified 32 core metabolites in seedlings subjected to PEG-mediated drought, 16 of which increased—including quercetin, isovitexin, cyanidin 3-O-beta-D-glucoside, L-arginine, and glycerophosphocholine, while the other 16 decreased—including 3-methoxytyramine, 2, 6-diaminopimelic acid, citric acid, UDP-alpha-D-glucose, adenosine, keto-D-fructose. The 32 core metabolites were enriched in 29 metabolic pathways, including lysine biosynthesis, citrate (TCA) cycle, anthocyanin biosynthesis, and aminoacyl-tRNA biosynthesis. Among them, taurine and hypotaurine metabolism, flavor and flavor biosynthesis, indole alkaline biosynthesis, and alanine, aspartate and glutamate metabolism were the four main metabolic pathways affected by drought. Our findings provide new insights into the physiological and metabolic response mechanisms of Tartary buckwheat to drought stress.

KEYWORDS

Tartary buckwheat; drought; untargeted metabolomics analysis; metabolic pathway; physiological response

1 Introduction

Drought is the most important environmental constraint to crop productivity and food security worldwide [1]. Water deficit has pronounced effects on plant growth, survival, physiology, and yield [2,3]. Plants subjected to drought undergo evident morphological modifications, including reduced shoot

growth (leaves and stems), and changes in root diameter, length, branches and lateral root formation, all of which disrupt plant–water relations and affect water-use efficiency [4,5]. Drought interferes with many physiological processes, including CO_2 assimilation and metabolism, ultimately leading to a significant reduction in biomass accumulation [6,7]. However, plants respond to drought through physiological and metabolic changes, such as inhibited transpiration through a reduction in leaf area or stomatal closure, to successfully minimize water loss [8]. Drought induces the production of reactive oxygen species (ROS) and modifies antioxidant systems [5,9]. Plants can improve their capacity for osmotic adjustment by accumulating solutes to maintain cell turgidity, protecting against cellular oxidative damage, and altering metabolic pathways to tolerate or resist water deficit [10,11]. Furthermore, the plant cell undergoes changes at the transcript, protein, and metabolite levels to acclimate to water deficit [11–14].

Metabolomics, also known as metabonomics or metabolic profiling, provides a useful and rapid method for assessing the changes occurring in the metabolome as a consequence of the environment [1,15–17]. It is a powerful tool for analyzing plant responses to environmental stimuli, by identifying changes in the profile of primary and secondary metabolites [15,18–20]. Primary metabolism, including carbon and nitrogen metabolism, is altered by drought. Primary carbon metabolites such as polyols and sugars, and nitrogen-storage metabolites such as quaternary ammonium compounds or amino acids, have been found to increase in response to drought, mainly in plant roots [20]. Secondary metabolites, produced by pathways derived from primary metabolic routes, also play an important role in the drought response [17,21]. Water stress has been reported to lead to increases in gamma-aminobutyric acid, trigonelline, cyanogenic glycosides, glucosinolates, terpenoids, alkaloids and condensed tannins [2,16]. Under drought stress, the flavonoid pathway regulates the production of reactive oxygen species (ROS) [21]. Of the root-specific metabolites, gamma-glutamyl compounds have been found to accumulate significantly in response to drought stress reflecting induction of the glutathione pathway [21]. Plant hormones, such as gibberellic acid, indoleacetic acid (auxin), ethylene, cytokinin, abscisic acid and brassinosteroids, as well as signaling compounds involved in hormone metabolism, have been widely studied for their involvement in the drought response [22–26]. ROS and reactive nitrogen species metabolism is active in drought-stressed roots, characterized by increased protein nitration and accumulation of nitric oxide and S-nitrosothiols in cortical cells [3]. In addition to elucidating the metabolic differences between developmental stages or organs, it is essential to achieve an integrated understanding of the whole-plant response [21].

Tartary buckwheat (*Fagopyrum tataricum*) is a traditional short-season pseudocereal crop in the family *Polygonaceae* [27] that contains diverse health-promoting compounds, such as flavonoids, anthocyanins, phenolics, amino acids and vitamins [28–30]. Tartary buckwheat is widely distributed in Asia, in the marginal lands of mountainous areas of Western China, the Himalayas, Japan and Korea, as well as in Europe and the Americas [27,31]. Tartary buckwheat grows in environments that are harsh and cold, with strong ultraviolet radiation and frequent and severe drought conditions in high-altitude mountainous areas, and in arid or semiarid regions, causing defective growth and yield loss of Tartary buckwheat. However, a lack of metabolic profiling seriously limits our understanding of the drought-responsive mechanisms in Tartary buckwheat. An elucidation of these mechanisms should indicate specific traits to be targeted in selection programs, and help in implementing crop-management practices under drought conditions. In this study, we provide insight into the mechanism of Tartary buckwheat responses to drought in terms of plant growth and metabolome profile.

2 Materials and Methods

2.1 Plant Materials and Site Description

F. tataricum variety Chuan Qiao No. 1(CQ1), one of the main varieties in China which is widely used for field production, was used in this experiment. The seeds were cultured in a special device with nutritional supply and then placed in a growth chamber (25°C). The special device was designed for seed

germination and growth under drought stress, without destroying the plant and allowing for seedling emergence [32]. For the water-deficit treatment, the 10-d-old Tartary buckwheat seedlings were treated with 25% (w/v) polyethylene glycol (PEG-6000) solution (Sigma-Aldrich, USA) for 3 days. Control plants were well-watered. Samples were collected from the aerial part of the seedlings in three independent biological replicates on days 1, 2 and 3 of the treatment for physiological index, while another six independent biological replicates were collected on day 2 of the treatment and immediately frozen in liquid nitrogen for metabolic profiling.

2.2 Sampling and Measurement Methods

2.2.1 Seedlings Growth, Biomass and Relative Water Content (RWC)

Stem lengths and main root lengths of 10 plants were recorded on day 3 of the treatment to calculate the ratio of root to stem length. Plants were oven-dried at 65°C until a constant weight was obtained. The average dry weight of 10 plants was calculated and expressed on a per plant basis (± SE). RWC was determined from fresh weight (FW), dry weight (DW), and turgid weight (TW) using the formula RWC (%) = [(FW-DW)/(TW-DW)] × 100 [33].

2.2.2 ROS Markers

Electrolyte leakage was measured by the method as described in a previous study [34]. The content of malondialdehyde (MDA) was measured using the thiobarbituric acid colorimetric reaction (TBARS) assay [35].

2.2.3 Extraction and Analysis of Activity of Antioxidant Enzymes

Superoxide dismutase (SOD) activity was measured as described in a previous study [36]. Peroxidase (POD) and catalase (CAT) activities were determined according to a previous study [37], and amylase activity was measured as described before [38].

2.2.4 Analysis of Osmotic Regulators

Soluble protein content was measured by Bradford protein assay, soluble sugar content was measured as described before [39], and proline (Pro) content was quantified spectrophotometrically [38].

2.2.5 Gas Chromatography–Mass Spectrophotometry (GC–MS) Analysis

A plant sample (100 mg) was placed in a 5 mL centrifuge tube. Five steel balls were placed in liquid nitrogen for 5 min. The tubes were placed in a highflux organization grinding apparatus set at 70 Hz for 1 min. Methanol (1000 µL precooled at −20°C) was added and the mixture was vortexed for 30 s. The tubes were then placed into an ultrasound machine at room temperature for 30 min. Later, 750 µL chloroform (precooled at −20°C) and 800 µL deionized water (4°C) were added to the tubes. Then the tubes were vortexed for 60 s, centrifuged for 10 min at 12 000 rpm (GIVE IN g) at 4°C. 1 mL of the supernatant was transferred to a new centrifuge tube. Samples were vacuum-concentrated and then dissolved in 250 µL aqueous methanol solution (1:1, 4°C), filtered through a 0.22-µm membrane, and submitted for LC–MS analysis. As a quality control, 20 µL was taken from each prepared sample extract and mixed (quality control samples were used to monitor deviations of the analytical results from these pooled mixtures and compare them to the errors caused by the analytical instrument itself). The rest of the sample was used for LC–MS detection.

Chromatographic separation was accomplished in an ACQUITY UPLC system equipped with an ACQUITY UPLC® HSS T3 (150 × 2.1 mm, 1.8 µm, Waters) column maintained at 40°C. The temperature of the autosampler was 4°C. Gradient elution of the analytes was carried out with 0.1% formic acid in water (A) and 0.1% formic acid in acetonitrile (B) at a flow rate of 0.25 mL min^{-1}. A 4-µL aliquot of the sample was injected after equilibration. An increasing linear gradient of solvent B (v/v) was used as follows: 0–1 min, 2% B; 1–9.5 min, 2%–50% B; 9.5–14 min, 50%–98% B; 14–15 min, 98% B; 15–15.5 min, 98%–2% B; 15.5–17 min, 2% B.

The HPLC-ESI-MSn experiments were executed in a Thermo LTQ–Orbitrap XL mass spectrometer with capillary voltages of 4.8 and 4.5 kV in negative (ESI−) and positive (ESI+) modes, respectively. Sheath gas and auxiliary gas were set at 45 and 15 arbitrary units, respectively. The capillary temperature was 325°C. The voltages of the capillary and tube were 35 and 50 V, and −15 and −50 V in positive and negative modes, respectively. The Orbitrap analyzer scanned over a mass range of m/z 89–1000 for full scan at a mass resolution of 60 000. Data-dependent acquisition in the MS/MS experiments was performed with collision-induced dissociation scan. The normalized collision energy was 30 eV. Dynamic exclusion was implemented with a repeat count of 2, and exclusion duration of 15 s.

2.3 Data Pretreatment and Multivariate Statistical Analysis

Data processing and analysis were performed according to Peng et al. [40] with slight modifications. The acquired MS data were analyzed by ChromaTOF software (v. 4.34, LECO, St. Joseph, MI). The dataset was normalized using the summed intensity of the peaks in each sample. In total, 546 peaks were detected in the tissues by GC–MS. The SIMCA-P + 13.0 software package (Umetrics, Umeå, Sweden) was used to analyze the GC–MS data. To visualize metabolic alterations in the experimental group, both unsupervised (principal component analysis, PCA) and supervised (orthogonal partial least squares discriminant analysis, OPLS-DA) segregation was exported. The parameters R2X(cum), R2Y(cum) and Q2(cum) were calculated to assess the quality of the models. After multivariate analysis, significant differences in each group were defined as having variable importance in projection (VIP) > 1.2, significance at $P < 0.05$ (t test) and fold change > 2; significantly altered metabolites were selected as candidates for further analysis.

2.4 Screening and Identification of Metabolic Differences

Differentially expressed compounds in the treatment group were selected by comparison to their control values using multivariate statistical method. Metabolites with both multivariate and univariate statistical significance (VIP > 1.0 and $P < 0.05$) were annotated with the aid of available reference standards in our laboratory, the NIST 05 standard mass spectral databases and the Feinh databases linked to ChromaTOF software. A similarity of > 70% was considered the reference standard. Based on the results of the enrichment, a customized vertical version of the histogram was created according to the significant vertical version of the top 10 entries in the column.

Statistical analyses were conducted using Excel 2010, SPSS 13.0 (Chicago, IL, USA) and SigmaPlot 10.0 (Aspire Software Intl., Ashburn, VA, USA). One-way ANOVA was used to determine the significance level, and means were compared by least significance difference (LSD) multiple comparison at a significance level of $P < 0.05$.

3 Results

3.1 Seedling Growth, Total Biomass, and RWC

Compared to the well-watered controls, the samples treated with PEG-induced drought showed significantly decreased shoot length but increased root length (Fig. 1A). Shoot biomass was significantly reduced by the drought treatment, whereas root biomass showed the opposite trend. The ratio of root-to-shoot biomass was therefore enhanced by drought (Fig. 1B). Under conditions of drought stress, seedling RWC decreased sharply, whereas that in the control seedlings showed no significant change during the 3 days of the experiment (Fig. 1C).

3.2 MDA Content and Electrolyte Leakage

Compared to the control plants, MDA content in the drought-treated seedlings was significantly higher (Fig. 2A). During the 3-day treatment, MDA content in drought-treated seedlings increased from day 0 to day

2, then decreased from day 2 to day 3. Electrolyte leakage increased significantly on all 3 days under PEG-induced drought conditions, whereas it did not change in the controls (Fig. 2B).
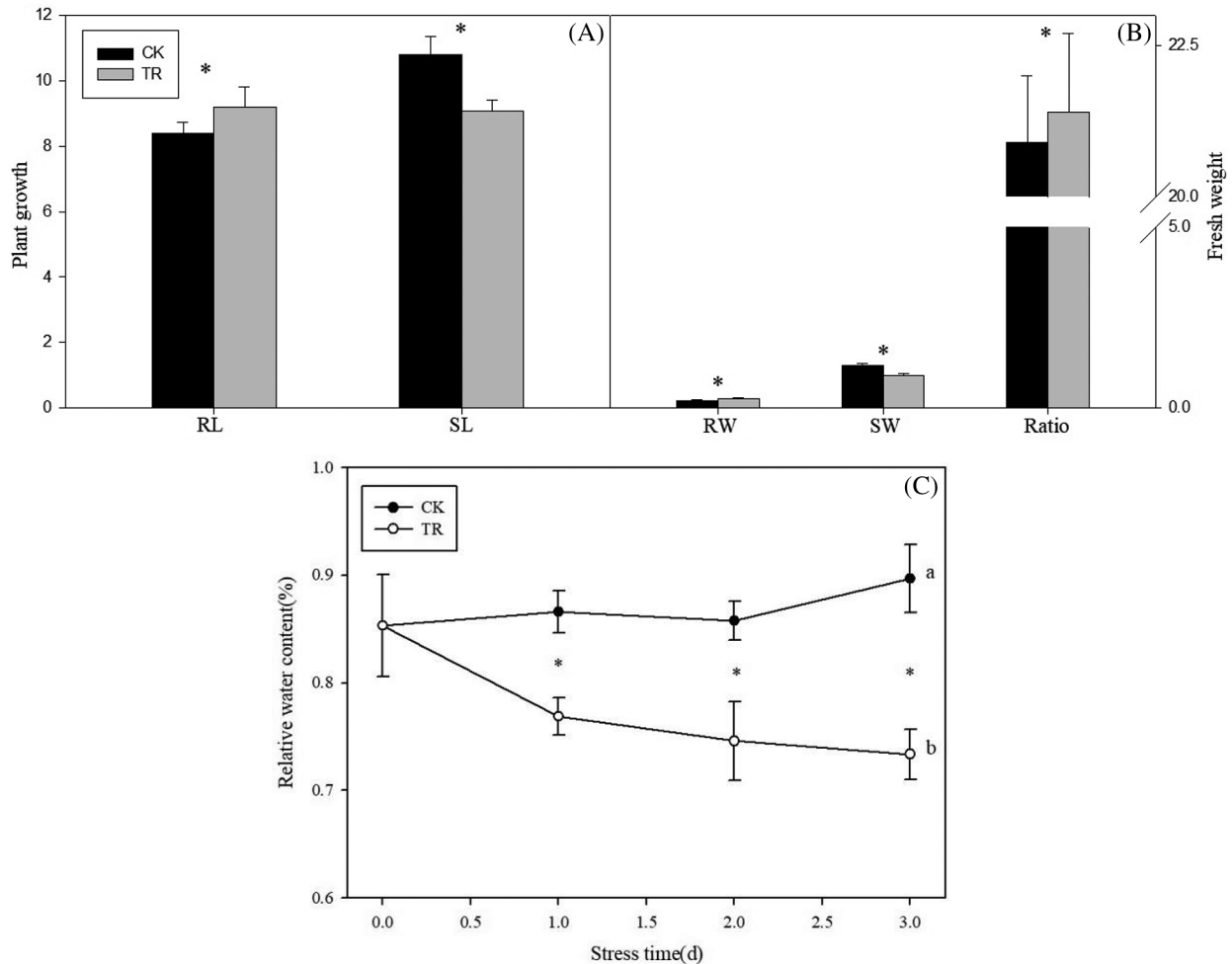

Figure 1: Mean (± SE) root length (RL) and shoot length (SL) (A), root weight (RW), shoot weight (SW) and the ratio between root and shoot (ratio) (B), and relative water content (RWC) (C) under drought stress treatment

Notes: Different lowercase letters indicate significant differences between treatments overall and asterisks (*) represent significant differences between well-watered (CK) and water-stressed (TR) plants on corresponding days ($P < 0.05$).

3.3 Activities of Antioxidant Enzymes and Amylase

Compared to the well-watered seedlings, SOD activity in the drought-treated seedlings was significantly higher on days 2 and 3 (Fig. 3A). Drought-stressed plants experienced a significant increase in POD activity compared to the well-watered controls on days 1 and 2 (Fig. 3B). CAT activity in the drought-treated seedlings was sharply elevated compared to the controls (Fig. 3C). Drought-stressed plants showed a significant increase in amylase activity compared to the well-watered controls over the 3 days of the experiment (Fig. 3D). During the 3-day period, SOD, POD, CAT and amylase activities of drought-stressed plants were highest on day 2.
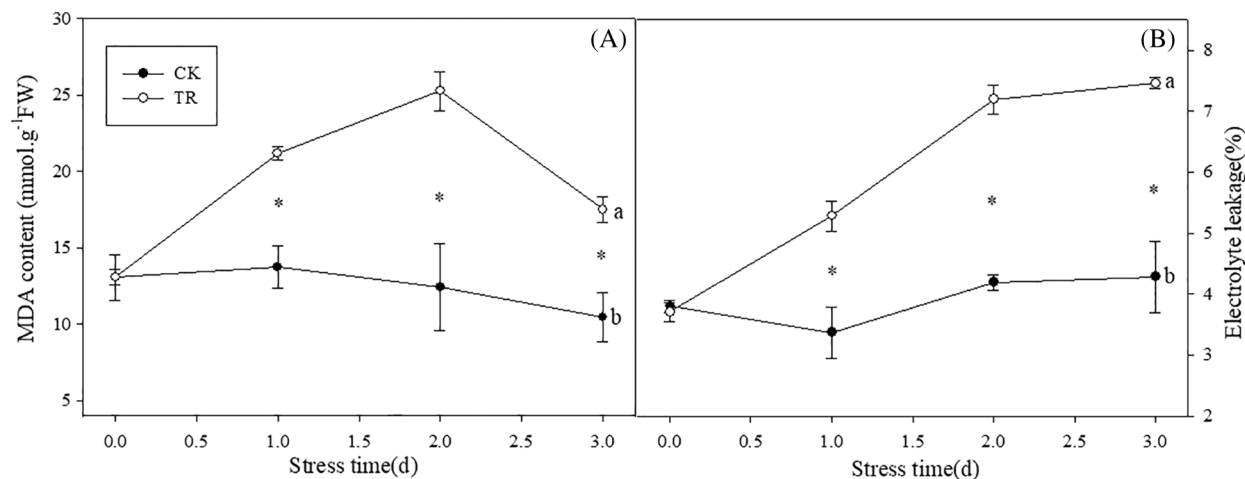
Figure 2: Mean (± SE) MDA content(A) and electrolyte leakage(B) under drought stress treatment
Note: Different lowercase letters indicate significant differences between treatments overall, and asterisks (*) represent significant differences between well-watered (CK) and water-stressed (TR) plants on corresponding days ($P < 0.05$).
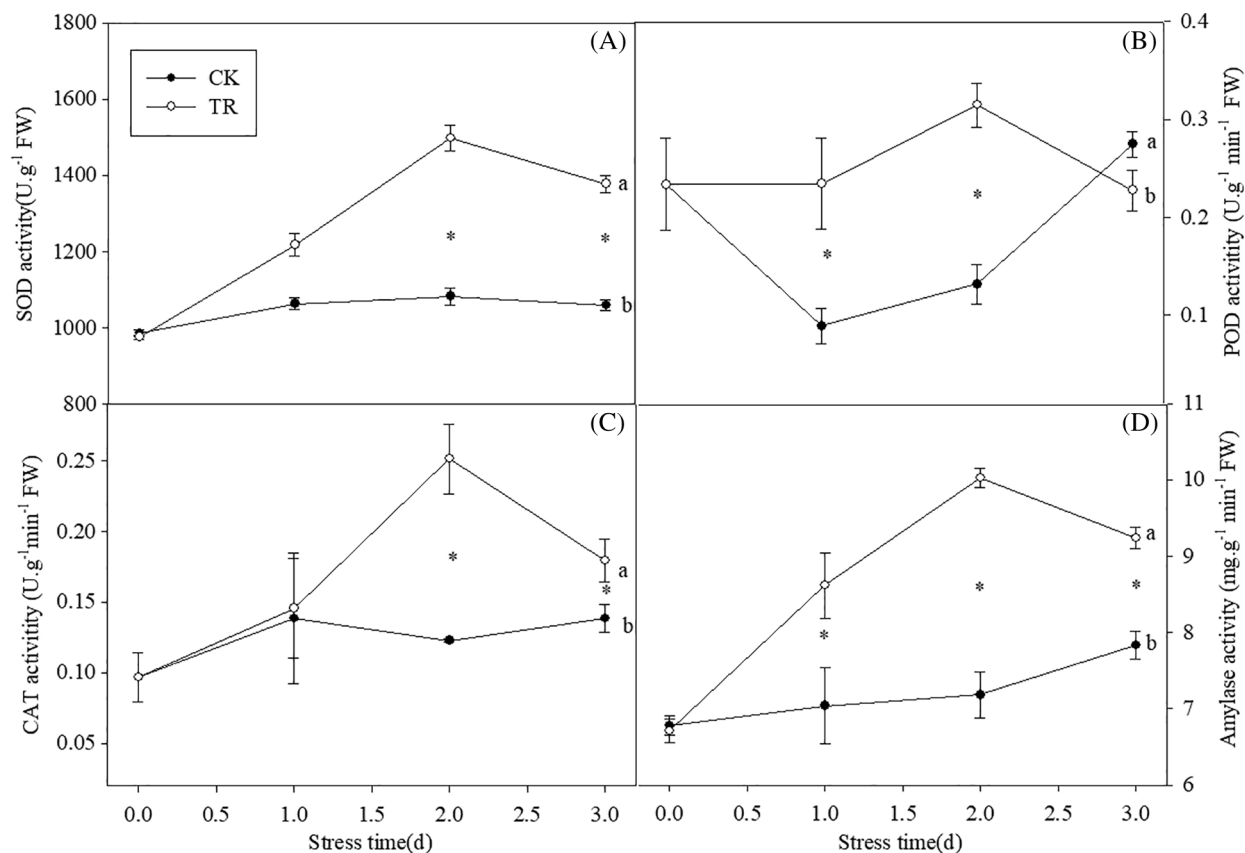

Figure 3: Mean (± SE) the SOD activity (A), POD activity (B), CAT activity (C) and amylase activity (D) under drought stress treatment
Note: Different lowercase letters indicate significant differences between treatments overall, and asterisks (*) represent significant differences between well-watered (CK) and water-stressed (TR) plants on corresponding days ($P < 0.05$).

3.4 Osmotic Regulators

Drought stress had stimulatory effects on soluble sugar, soluble protein and Pro contents (Figs. 4A–4C). Soluble sugar content of drought-stressed seedlings was significantly higher than that of controls on days 1 and 2. Compared to the controls, soluble protein content was enhanced by drought treatment on all days, whereas Pro content increased on days 2 and 3. During the 3 days of the experiment, soluble sugar, soluble protein and Pro contents in the drought-treated seedlings were highest on day 2.
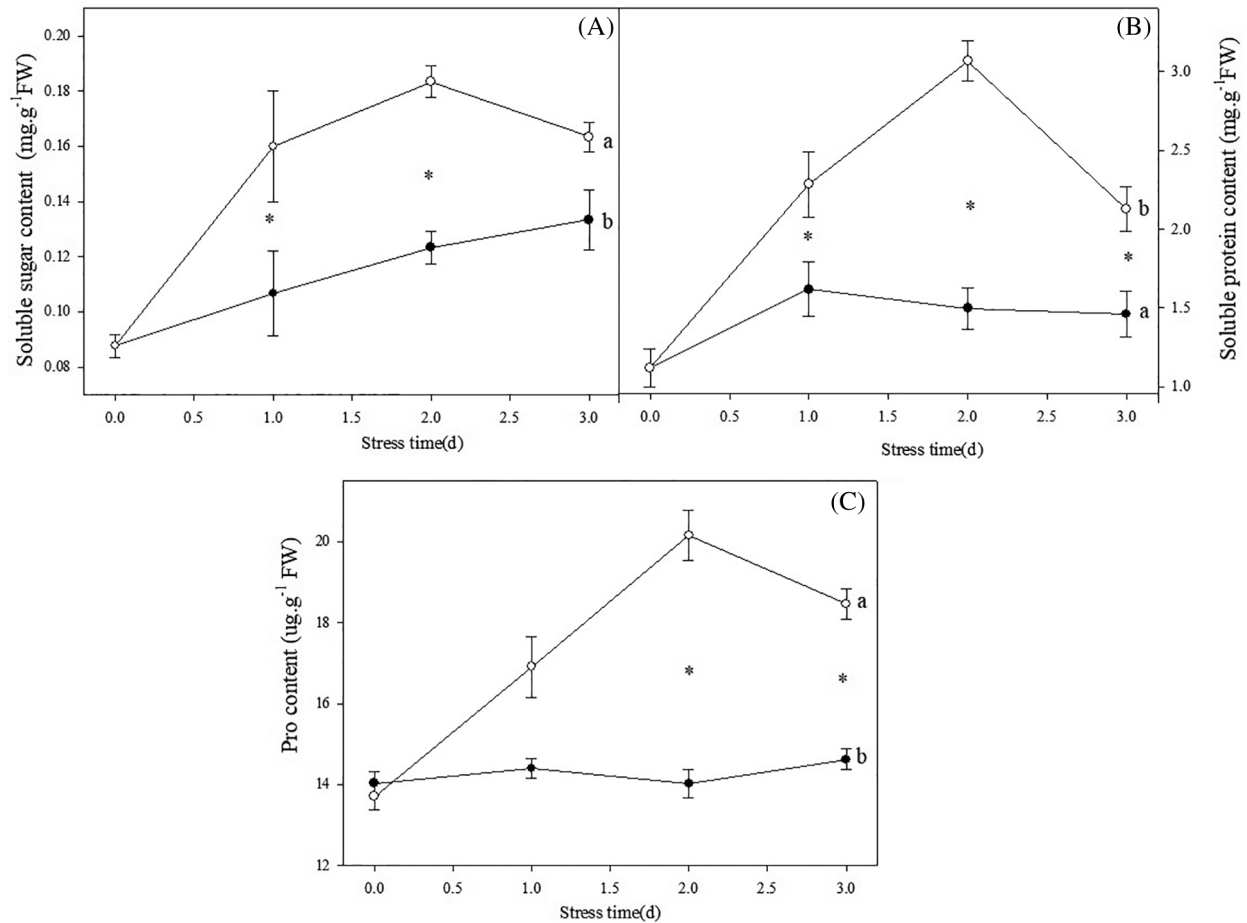

Figure 4: Mean (± SE) of the soluble sugar content (A), the soluble protein content (B), and Pro content (C) under drought stress treatment

Note: Different lowercase letters indicate significant differences between treatments overall, and asterisks (*) represent significant differences between well-watered (CK) and water-stressed (TR) plants on corresponding days ($P < 0.05$).

3.5 Metabolic Changes Caused by Drought

3.5.1 Identification of Differentially Expressed Metabolites

GC–MS was used for maximal separation of the wide range of metabolites present in the drought-treated seedlings. In total, 1017 differentially expressed metabolites were identified in the drought-treated compared to control treatments (592 increased and 425 decreased) comprising organic acids, sugars, sugar alcohols, fatty acids, amino acids, flavones, sterols and phospholipids, as identified using the NIST library.

PCA was performed using the six individual replicates from each comparison group. The two principal components could explain 54.1% and 54.7% of the variation between drought-treated and control seedlings for the negative and positive ESI modes, respectively (Figs. 5A and 5B). By OPLS-DA, the two principal components explained 53.4% and 50.0% of the variation between treated and control seedlings for the negative and positive ESI modes, respectively (Figs. 5C and 5D). To test for model reproducibility and model fit, response-sorting tests of the OPLS-DA model, namely, fixed X matrix and previously defined Y matrix variable classifications (i.e., 0 or 1) were randomly arranged. The OPLS-DA model was established to obtain the corresponding stochastic model of R2 and Q2 values. With the original model of R2Y and Q2Y linear regression, the regression line and the Y axis intercept values (R2 and Q2) were used to measure whether the model was over-fitted (Figs. 5E and 5F). The model remained valid after cross-validation.

3.5.2 Metabolic Profiles and key Metabolites Affected by Drought

For the metabolomics analysis, 32 core metabolites of Tartary buckwheat were identified and quantified (Table 1, Fig. 6). A heat map showed overall changes in the 32 metabolites under normal *vs.* drought conditions (Fig. 7). Among them, quercetin, isovitexin, cyanidin 3-O-beta-D-glucoside, L-arginine, glycerophosphocholine, L-aspartic acid, tryptamine, (-)-epicatechin, taurine, quercetin 3-O-beta-D-glucopyranoside, N-acetyl-D-phenylalanine, carprofen, 2-deoxy-alpha-D-ribopyranose, 1-aminocyclobutane carboxylic acid, dimethyl phthalate, L-asparagine, and 2-dehydro-D-gluconic acid accumulated in the drought-treated seedlings (Figs. 6 and 7). The compounds 3-methoxytyramine, 2, 6-diaminopimelic acid, citric acid, UDP-alpha-D-glucose, adenosine, keto-D-fructose, enterolactone, L-pipecolic acid, erbstatin analog, vanillylmandelic acid, UMP, fumaric acid, CMP, galactitol, and thio-m-toluthioamide showed higher accumulations in the well-watered seedlings (Figs. 6 and 7).

Results show log2 fold change ratios; red indicates an upregulation; green indicates a down-regulation. Color intensity codes are given in the color bar at the right side of the figures. Different clusters containing the metabolites with the same behavior are outlined.

3.5.3 Metabolic Pathways Affected by Drought

The 32 core metabolites were enriched in 29 metabolic pathways (Table 2). The pathways included alanine, aspartate and glutamate metabolism, flavone and flavonol biosynthesis, lysine biosynthesis, citrate cycle (TCA cycle), anthocyanin biosynthesis, aminoacyl-tRNA biosynthesis, pyrimidine metabolism, zeatin biosynthesis, and purine metabolism. With fold change > 0.2 as the screening condition, the KEGG metabolic pathways taurine and hypotaurine metabolism, flavor and flavor biosynthesis, indole alkaline biosynthesis, and alanine, aspartate and glutamate metabolism were most highly represented.

4 Discussion

Tartary buckwheat is an important pseudocereal crop worldwide. Due to its limited growing area, Tartary buckwheat is typically exposed to a number of environmental stresses, such as high light/UV radiation, cold, drought, salt, and heavy metals. Drought severely affects growth and yield of Tartary buckwheat in agricultural production. Unfortunately, little is known about the effect of drought on Tartary buckwheat and its response to water stress. This motivated the current study.
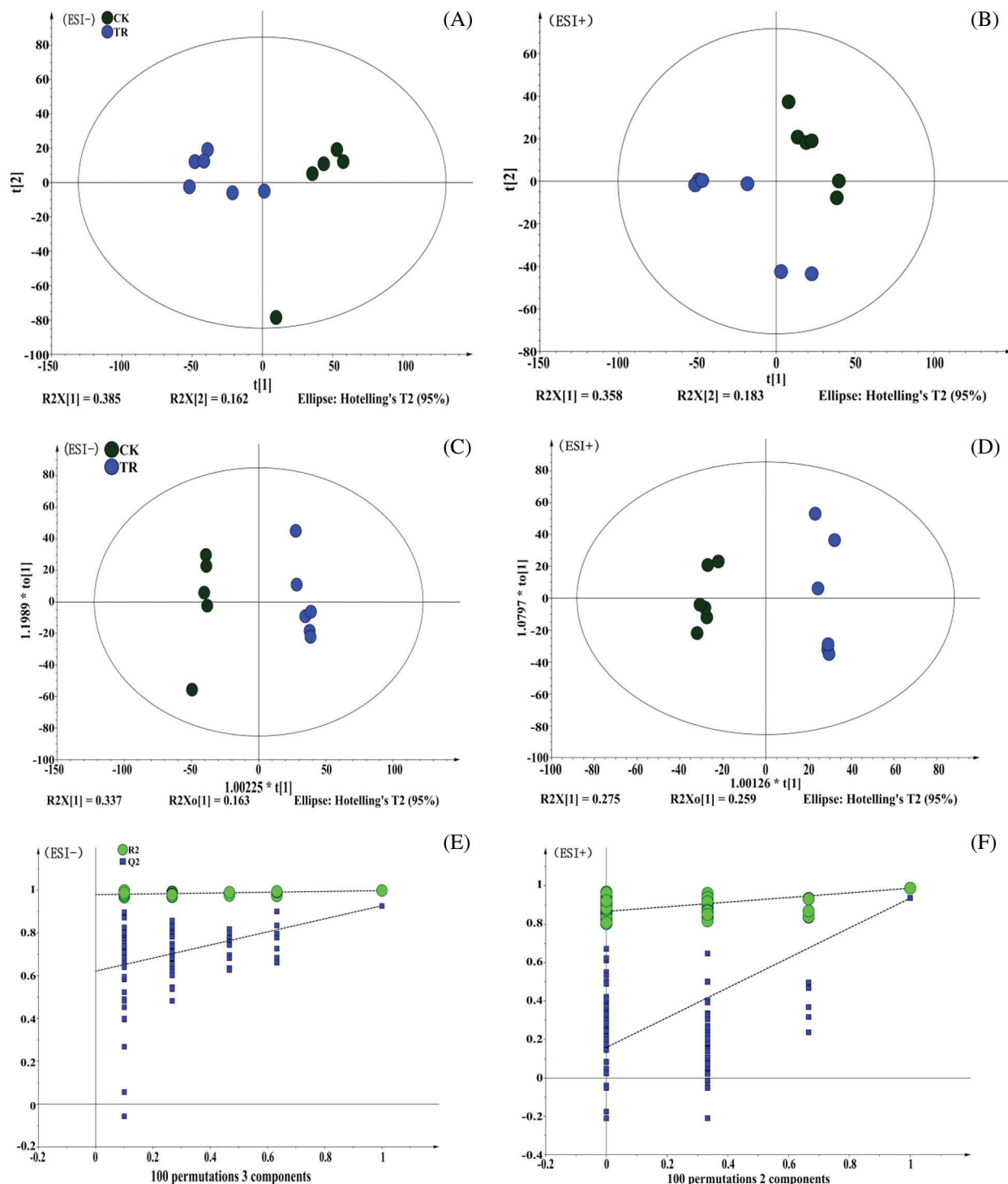
Figure 5: Principal component analysis (PCA) score plots of all samples (ESI-and ESI+) for the negative (A) and positive (B) ESI modes, PLS-DA score plots for the negative (C) and positive (D) ESI modes, permutation test for the negative (E) and positive (F) ESI modes. Each data point represents an independent sample

Table 1: Relative retention times (RT) and mass-to-charge (m/z) ratios used for identification and quantification of metabolites in Tartary buckwheat

| No.	Metabolites	m/z	rt	exact_mass	formula	KEGG	log2fc_TR/CK	precursor_type
1	L-Asparagine	131.05	86.0212	132.1180	C4H8N2O3	C00152	1.1363	[M–H]–
2	2-Dehydro-D-Gluconic acid	193.03	92.9880	194.1394	C6H10O7	C06473	2.0021	[M–H]–
3	Adenosine	265.95	597.4320	267.2415	C10H13N5O4	C00212	−1.0686	[M–H]–
4	Keto-D-Fructose	180.08	94.1706	180.1559	C6H12O6	C10906	−0.6756	[M+H]+
5	Dimethyl Phthalate	195.06	532.5050	194.1840	C10H10O4	C11233	0.6326	[M+H]+
6	Erbstatin Analog	195.06	62.5494	194.0579	C10H10O4		−1.3432	[M+H]+
7	Enterolactone	297.12	828.3370	298.3331	C18H18O4	C18165	−1.6725	[M–H]–
8	L-Pipecolic acid	129.13	63.3667	129.1570	C6H11NO2	C00408	−1.2225	[M+H]+
9	Thio-M-Toluthioamide	152.05	121.0800	151.0456	C8H9NS		−1.7139	[M+H]+
10	Glycerophosphocholine	258.11	90.4775	257.2213	C8H20NO6P	C00670	2.9092	[M+H]+
11	2, 6-Diaminopimelic acid	191.10	95.4345	190.1971	C7H14N2O4	C00666	−0.6425	[M+H]+
12	1-Aminocyclobutane Carboxylic acid	116.07	801.2960	115.0633	C5H9NO2		0.7925	[M+H]+
13	Tryptamine	161.11	353.0490	160.2157	C10H12N2	C00398	2.2547	[M+H]+
14	Quercetin 3-O-Beta-D-Glucopyranoside	463.09	435.8050	464.3763	C21H20O12	C05623	2.2074	[M–H]–
15	Galactitol	180.97	246.3455	182.1718	C6H14O6	C01697	−2.2208	[M–H]–
16	N-Acetyl-D-Phenylalanine	206.08	437.9250	207.2259	C11H13NO3	C05620	1.9778	[M–H]–
17	CMP	324.21	63.5064	323.1966	C9H14N3O8P	C00055	−1.7152	[M+H]+
18	Isovitexin	431.09	562.7225	432.3775	C21H20O10	C01714	1.5859	[M–H]-
19	L-Aspartic acid	134.04	90.2994	133.1027	C4H7NO4	C00049	0.9493	[M+H]+
20	L-Arginine	173.10	83.7531	174.2010	C6H14N4O2	C00062	1.0549	[M–H]–
21	UMP	324.21	175.6980	324.1814	C9H13N2O9P	C00105	−1.0019	[M+H]+
22	Carprofen	272.05	437.9310	273.0557	C15H12ClNO2	C18364	1.6589	[M–H]–
23	Cyanidin 3-O-Beta-D-Glucoside	447.09	489.2090	449.3848	C21H21O11	C08604	0.8494	[M–H]–
24	3-Methoxytyramine	168.10	255.8320	167.2050	C9H13NO2	C05587	−0.8316	[M+H]+
25	Citric acid	191.02	234.6480	192.1235	C6H8O7	C00158	−1.0111	[M–H]–
26	(-)-Epicatechin	289.07	385.8055	290.2681	C15H14O6	C09727	0.6699	[M–H]–
27	Quercetin	301.03	621.1610	302.2357	C15H10O7	C00389	0.9482	[M–H]–
28	2-Deoxy-Alpha-D-Ribopyranose	133.05	167.6620	134.1305	C5H10O4	C08347	0.7191	[M–H]–
29	Taurine	125.99	76.3770	125.1480	C2H7NO3S	C00245	1.5265	[M+H]+
30	UDP-Alpha-D-Glucose	565.04	88.0347	566.3018	C15H24N2O17P2	C00029	−0.8916	[M–H]–
31	Vanillylmandelic acid	199.17	368.9600	198.1727	C9H10O5	C05584	−0.6603	[M+H]+
32	Fumaric acid	117.09	196.0650	116.0722	C4H4O4	C00122	−0.6170	[M+H]+
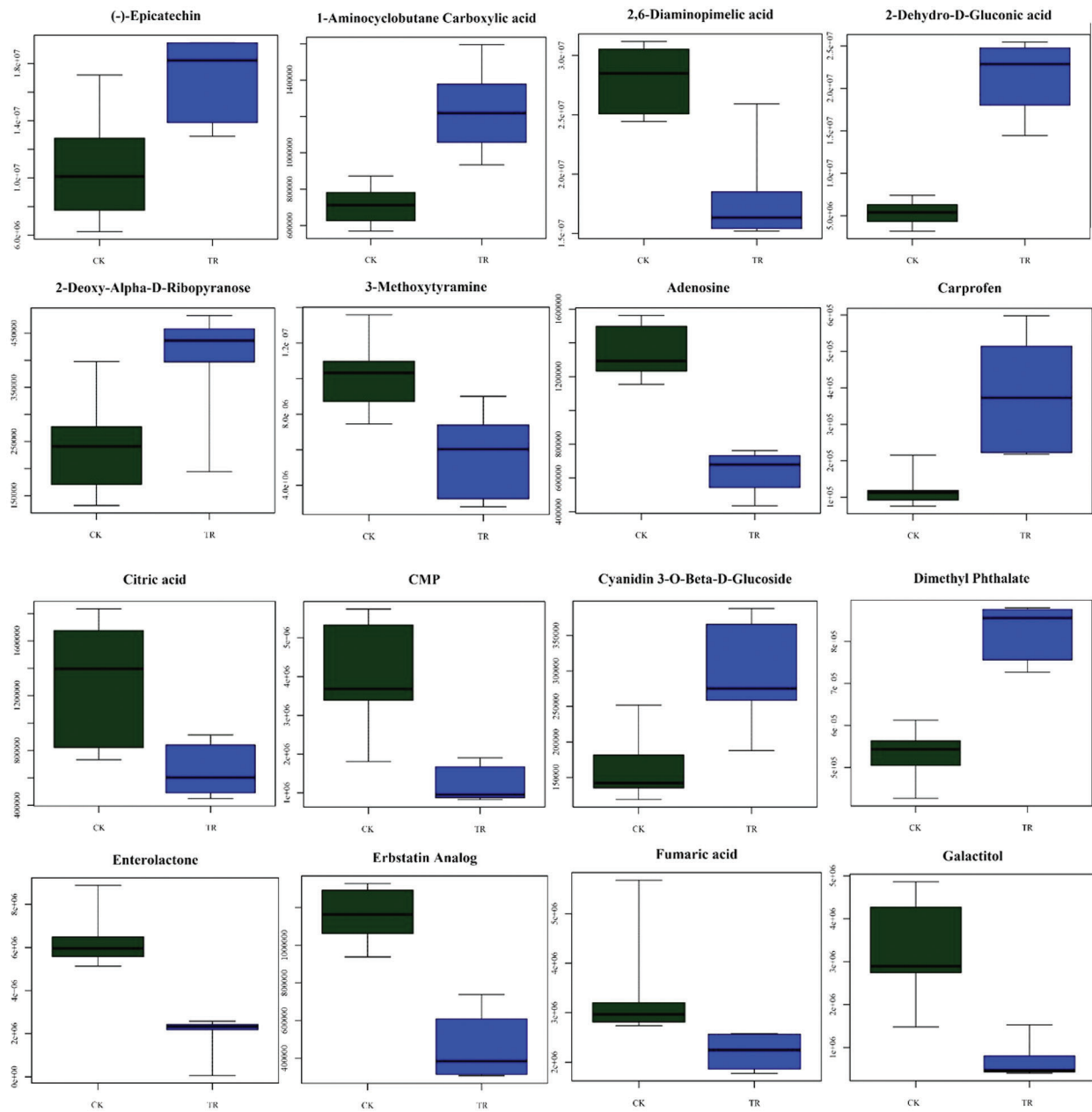
Figure 6: (Continued)
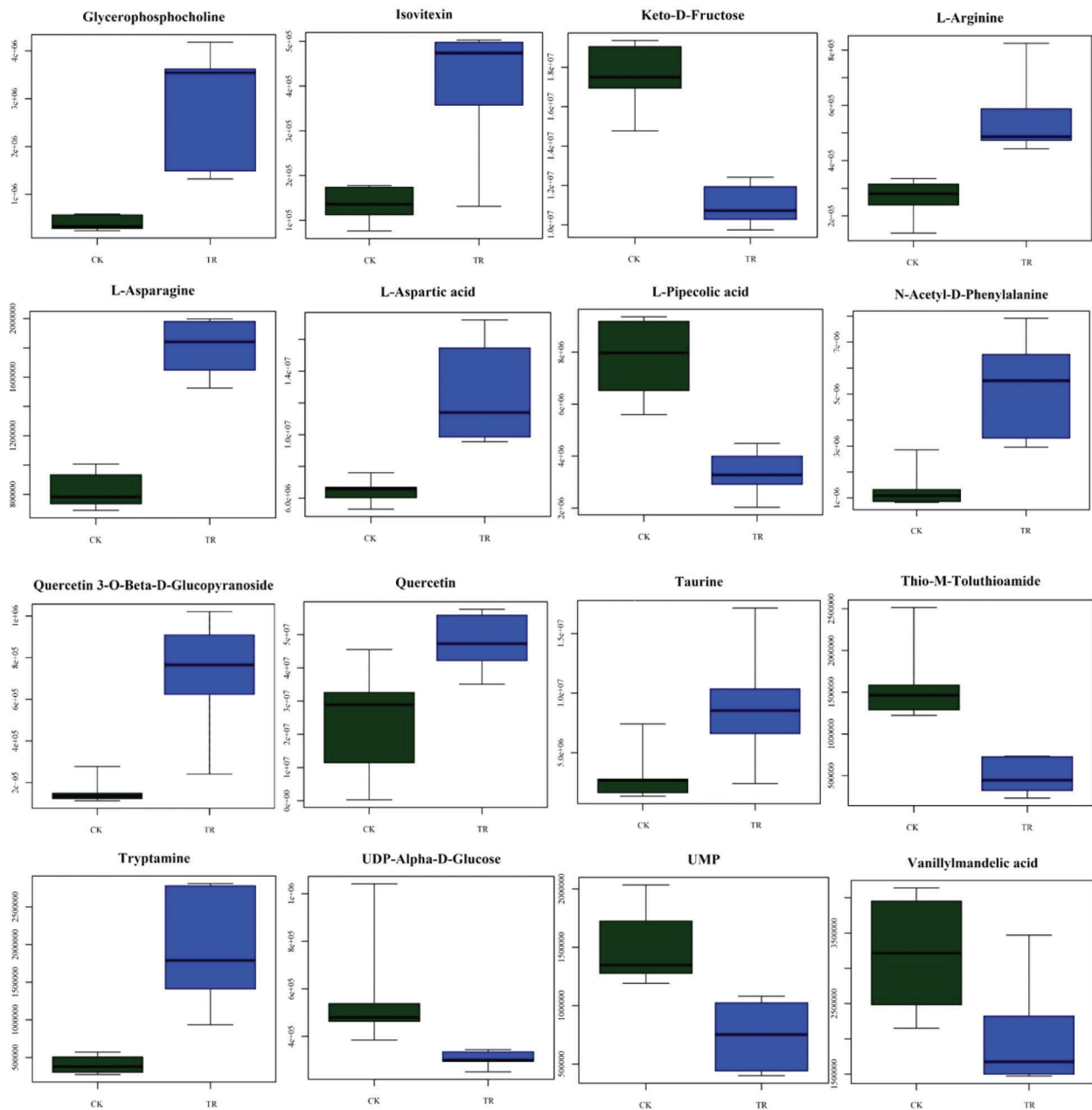
Figure 6: Metabolites changes in Tartary buckwheat at 2 days after treatment. Green histograms correspond to the control and blue histograms to the treatment
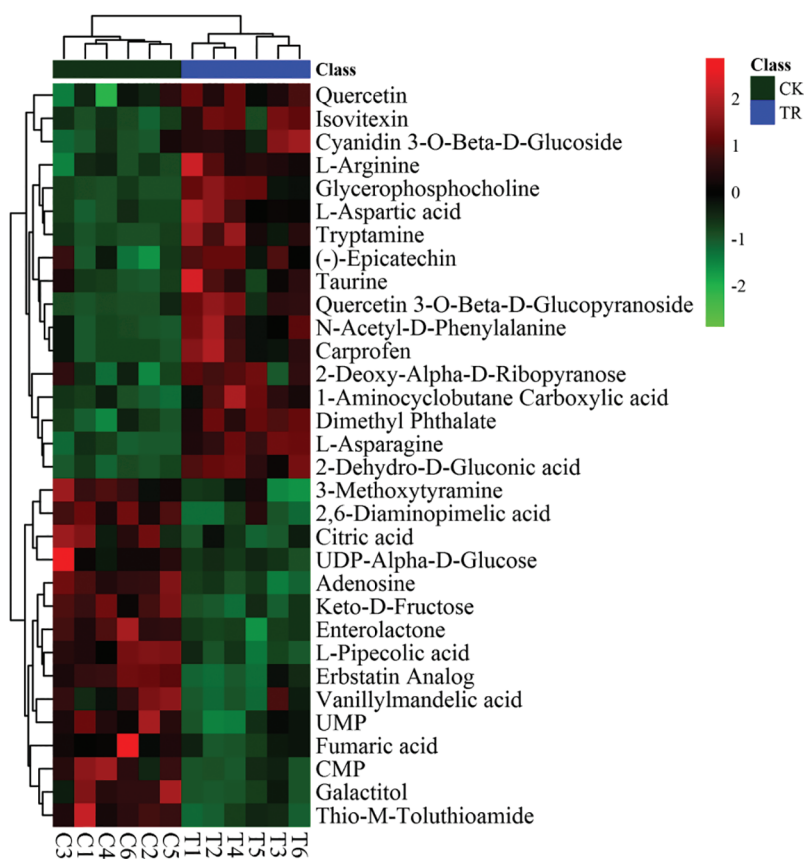
Figure 7: Heat map of changes in 32 metabolites in Tartary buckwheat at 2 days after treatment

Table 2: Metabolite-related pathways

	Total	Hits	−log(p)	Impact	Compounds	Pathway
Alanine, aspartate and glutamate metabolism	22	3	4.4347	0.2069	C00049, C00152, C00122	ath00250
Flavone and flavonol biosynthesis	9	2	4.1362	0.64	C00389, C05623	ath00944
Lysine biosynthesis	10	2	3.927	0.16667	C00666, C00049	ath00300
Arginine and proline metabolism	38	3	2.9755	0.10731	C00049, C00062, C00122	ath00330
Citrate cycle (TCA cycle)	20	2	2.6254	0.12905	C00158, C00122	ath00020
Taurine and hypotaurine metabolism	5	1	2.2277	1	C00245	ath00430
Indole alkaloid biosynthesis	7	1	1.9127	0.4	C00398	ath00901
Anthocyanin biosynthesis	8	1	1.7899	0	C08604	ath00942
Aminoacyl-tRNA biosynthesis	67	3	1.6699	0	C00152, C00062, C00049	ath00970
Pyrimidine metabolism	38	2	1.5619	0.11976	C00105, C00055	ath00240
Cyanoamino acid metabolism	11	1	1.5035	0	C00049	ath00460

(Continued)

Table 2 (continued)

	Total	Hits	−log(p)	Impact	Compounds	Pathway
beta-Alanine metabolism	12	1	1.427	0	C00049	ath00410
Nicotinate and nicotinamide metabolism	12	1	1.427	0	C00049	ath00760
Pentose and glucuronate interconversions	12	1	1.427	0.1	C00029	ath00040
Flavonoid biosynthesis	43	2	1.3783	0.00137	C00389, C09727	ath00941
Glycerolipid metabolism	13	1	1.3575	0	C00029	ath00561
Ascorbate and aldarate metabolism	15	1	1.2354	0	C00029	ath00053
Glyoxylate and dicarboxylate metabolism	17	1	1.1311	0.10544	C00158	ath00630
Tyrosine metabolism	18	1	1.0844	0	C00122	ath00350
Zeatin biosynthesis	19	1	1.0406	0.00435	C00029	ath00908
Carbon fixation in photosynthetic organisms	21	1	0.96111	0	C00049	ath00710
Glycerophospholipid metabolism	25	1	0.82746	0.02342	C00670	ath00564
Galactose metabolism	26	1	0.79833	0.02039	C00029	ath00052
Tryptophan metabolism	27	1	0.77064	0.06471	C00398	ath00380
Glycine, serine and threonine metabolism	30	1	0.69521	0	C00049	ath00260
Starch and sucrose metabolism	30	1	0.69521	0.17308	C00029	ath00500
Cysteine and methionine metabolism	34	1	0.60945	0	C00049	ath00270
Amino sugar and nucleotide sugar metabolism	41	1	0.48981	0.1527	C00029	ath00520
Purine metabolism	61	1	0.27576	0.00256	C00212	ath00230

4.1 Seedling Growth, Physiological and Biochemical Indexes

Previous research has shown the many adverse effects of drought stress on plant growth, physiological metabolism and biochemical parameters [41], ultimately resulting in yield reduction or even plant death [42,43] . We found a significant reduction in shoot biomass and shoot length of Tartary buckwheat plants under drought, indicating inhibition of plant shoot growth under the drought treatment, as reported in wheat and other plants [44]. However, root length increased under drought, confirming the accessibility of moisture deep in the soil and ensuring adaptation to drought stress. The observed decline of RWC under water stress can damage the plant's ability to maintain its water balance [45]. Stressed plants exhibit excess generation of ROS which can cause membrane lipid peroxidation, leading to cell damage or death [46]. Enhanced H_2O_2, MDA contents and electrolyte leakage are common symptoms of membrane damage under water stress [45,47]. MDA is the final product of membrane lipid peroxidation and indicates cell membrane injury [35], and electrolyte leakage is considered a marker of membrane damage under drought [47]. In our study, MDA and electrolyte leakage were significantly increased in the treated compared to control seedlings, indicating that drought can result in membrane damage; significant differences in MDA content and electrolyte leakage appeared at 24 h into the drought treatment.

To alleviate drought-induced oxidative stress, antioxidant enzymes function as ROS scavengers [47]. SOD is the first enzyme to play a key role in oxidative defense by catalyzing superoxide free radical dismutation of O_2^- to H_2O_2 [48]; the generated H_2O_2 is then eliminated by CAT and POD [47,49] through its catalysis to H_2O and O_2 [45]. SOD activity in Tartary buckwheat increased significantly 24 h after drought induction, and continued to increase to 48 h of drought. Significant increases in POD and CAT activity have been shown in stressed plants [45]. POD and CAT activity in Tartary buckwheat showed the same trend as SOD activity under the drought treatment. Increases in SOD, POD and CAT activities in Tartary buckwheat after rehydration could reflect an adaptation toward alleviating oxidative stress and improving growth, as in other plants [50].

Typically, osmotically active solutes such as Pro, soluble proteins and soluble sugars can mitigate the oxidative damage caused by ROS under water stress [51]. These molecules stimulate plants to absorb more water to withstand dehydration by maintaining turgor, buffering against ROS and protecting the redox balance [51] . Among them, Pro exhibits antioxidant activity and promotes redox to maintain homeostasis, thereby reducing lipid peroxidation [52]. The Pro content of Tartary buckwheat showed a significant and remarkable increase under drought stress 48 h after drought initiation. Plant accumulation of soluble proteins and soluble sugars under drought stress has been found in many studies [48]. Here, the contents of these two osmotic-adjustment substances showed the same trends, mitigating drought damage.

4.2 Secondary Metabolites and Pathways

Plants tend to biosynthesize specialized metabolites to adapt to drought stress. We identified 32 core metabolites that were enriched in 29 metabolic pathways in a Tartary buckwheat variety CQ1. Of these core metabolites, taurine accumulated significantly in response to drought stress (Fig. 6). In plants, an increase in taurine reflects induction of the taurine and hypotaurine metabolic pathway (Table 2). Taurine plays an important role in adjusting normal physiological functions to confer stress resistance via osmotic regulation or antioxidation [53].

Flavonoids are postulated to contribute antioxidant protection, due to their hydroxyl groups, the presence of double bonds, and their predisposition toward glycosylation and methylation [54]. Quercetin is considered one of the best electron donors among the flavonoids as it has an ortho-dihydroxy pattern in the B-ring of the flavonoid skeleton [55]. In Tartary buckwheat, we found quercetin to be associated with quercetin 3-O-beta-D-glucopyranoside in flavone and flavonol biosynthesis improved under drought conditions (Fig. 6, Table 2), and the increase in quercetin concentration conferred greater $H_2O_2^-$ scavenging activity [56], which might be a strategy for drought tolerance due to the powerful antioxidant activity of flavonoids [57].

Tryptophan is the substrate for alkaloids, indoles, auxin, phytomelatonin, glucosinolates and phytoalexins, and it therefore plays an important role in the plant stress response [58]. Tryptamine is biosynthesized from tryptophan by trytophan decarboxylase and oxidized by monoamine oxidase [59]. Tryptamine is one of the major contributors to the water-stress response in barley [60]. In rice, the indole alkaloid tryptamine inhibited infection by *Magnaporthe oryzae* as a key factor in light-enhanced resistance [59]. In Tartary buckwheat, tryptamine increased through the indole alkaline biosynthesis pathway under drought conditions.

The accumulation of amino acids has been reported in various plants under abiotic stress. They are considered to have a beneficial effect during stress acclimation in some species, or to indicate cell damage in others [61,62]. In maize, arginine was considered an osmoprotectant as it increased under water stress [61]. In a *Fagus sylvatica* L. population, aspartic acid together with valine, isoleucine, threonine, serine and glycine, increased in response to water stress [63]. In our study, L-aspartic acid and

L-asparagine involved in alanine, aspartate and glutamate metabolism were upregulated under drought conditions, whereas fumaric acid decreased.

5 Conclusion

To our knowledge, this is the first study of physiological responses and identification of the metabolic profile of Tatary buckwheat under drought stress. ROS markers, including MDA content and electrolyte leakage, activities of the antioxidant enzymes SOD, POD and CAT, and contents of the osmotic regulators soluble sugar, soluble protein and Pro all increased in response to drought stress in Tatary buckwheat, along with metabolites that included organic acids, sugars, sugar alcohols, fatty acids, amino acids, flavones, sterols and phospholipids. Taurine and hypotaurine metabolism, flavone and flavonol biosynthesis, indole alkaline biosynthesis, alanine, aspartate and glutamate metabolism might be the main metabolic pathways used to cope with drought stress. The presented information on the metabolic profile should provide new insights into the biochemical pathways underlying drought tolerance in Tartary buckwheat plants.

Conflicts of Interest: The authors declare that they have no conflicts of interest to report regarding the present study.

References

1. Omena-Garcia, P. P., Oliveira, M., Medeiros, D. B., Vallarino, J. G., Ribeiro, D. M. et al. (2019). Growth and metabolic adjustments in response to gibberellin deficiency in drought stressed tomato plants. *Environmental and Experimental Botany, 159,* 95–107. DOI 10.1016/j.envexpbot.2018.12.011.

2. Charlton, A. J., Donarski, J. A., Harrison, M., Jones, S. A., Godward, J. et al. (2008). Responses of the pea (*Pisum sativum* L.) leaf metabolome to drought stress assessed by nuclear magnetic resonance spectroscopy. *Metabolomics, 4,* 312. DOI 10.1007/s11306-008-0128-0.

3. Santiago, S., Corpas, F. J., Marta, R. R., Raquel, V., Barroso, J. B. et al. (2019). Drought stress triggers the accumulation of NO and SNOS in cortical cells of *Lotus japonicus* L. rootsand the nitration of proteins with relevant metabolic function. *Environmental and Experimental Botany, 161,* 228–241. DOI 10.1016/j.envexpbot.2018.08.007.

4. Lynch, J. P., Chimungu, J. G., Brown, K. M. (2014). Root anatomical phenes associated with water acquisition from drying soil: Targets for crop improvement. *Journal of Experimental Botany, 65,* 6155–6166. DOI 10.1093/jxb/eru162.

5. Ye, H., Manish, R., Babu, V., Zhou, L., Chen, P. Y. et al. (2018). Genetic diversity of root system architecture in response to drought stress in grain legumes. *Journal of Experimental Botany, 697,* 3267–327. DOI 10.1093/jxb/ery082.

6. Flexas, J., Bota, J., Loreto, F., Cornic, G., Sharkey, T. D. (2004). Diffusive and metabolic limitations to photosynthesis under drought and salinity in C$_3$ plants. *Plant Biology, 6,* 269–279. DOI 10.1055/s-2004-820867.

7. Farooq, M., Wahid, A., Kobayashi, N., Fujita, D., Basra, S. (2009). Plant drought stress: Effects, mechanisms and management. *Agronomy for Sustainable Development, 29,* 185–212. DOI 10.1051/agro:2008021.

8. Claeys, H., Inze, D. (2013). The agony of choice: How plants balance growth and survival under water-limiting conditions. *Plant Physiology, 162,* 1768–1779. DOI 10.1104/pp.113.220921.

9. Xu, Y., Burgess, P., Zhang, X., Huang, B. (2016). Enhancing cytokinin synthesis by overexpressing IPT alleviated drought inhibition of root growth through activating ROS-scavenging systems in agrostis stolonifera. *Journal of Experimental Botany, 67,* 1979–1992. DOI 10.1093/jxb/erw019.

10. Carla, P., Maria, M. C., Ricardo, C. P. (2001). Alterations in carbon and nitrogen metabolism induced by water deficit in the stems and leaves of *Lupinus albus* L. *Journal of Experimental Botany, 52,* 1063–1070. DOI 10.1093/jexbot/52.358.1063.

11. Shulaev, V. C., Miller, G., Mittler, R. (2008). Metabolomics for plant stress response. *Physiology Plantarum, 132,* 199–208. DOI 10.1111/j.1399-3054.2007.01025.x.

12. Ahuja, I., Vos, R. D., Bones, A. M., Hall, R. D. (2010). Plant molecular stress responses face climate change. *Trends Plant Science, 15,* 664–674. DOI 10.1016/j.tplants.2010.08.002.

13. Chae, L., Sudat, S., Dudoit, S., Zhu, T., Luan, S. (2009). Diverse transcriptional programs associated with environmental stress and hormones in the arabidopsis receptor-like kinase gene family. *Molecular Plant, 2,* 84–107. DOI 10.1093/mp/ssn083.

14. Yates, S. A., Swain, M. T., Hegarty, M. J., Chernukin, I., Lowe, M. et al. (2014). De novo assembly of red clover transcriptome based on RNA-SEQ data provides insight into drought response, gene discovery and marker identification. *BMC Genomics, 15,* 453–453. DOI 10.1186/1471-2164-15-453.

15. Cai, X., Sun, X. G., Che, N. X., Fu, J. Q., Zhang, Y. L. (2016). Metabolic and growth responses of maize to successive drought and re-watering cycles. *Agricultural Water Management, 172,* 62–73. DOI 10.1016/j.agwat.2016.04.016.

16. Pan, L., Chen, M., Wang, J., Ma, X., Fan, X. et al. (2018). Integrated omics data of two annual ryegrass (*Lolium multiflorum* L.) genotypes reveals core metabolic processes under drought stress. *BMC Plant Biology, 18,* 26–42. DOI 10.1186/s12870-018-1239-z.

17. Xiong, Q., Cao, C., Shen, T., Zhong, L., He, H. H. et al. (2019). Comprehensive metabolomic and proteomic analysis in biochemical metabolic pathways of rice spikes under drought and submergence stress. *BBA-Proteins & Proteomic, 1967,* 237–247. DOI 10.1016/j.bbapap.2019.01.001.

18. Warren, C. R., Aranda, I., Cano, F. J. (2011). Responses to water stress of gas exchange and metabolites in eucalyptus and acacia spp. *Plant Cell and Environment, 34,* 1609–1629. DOI 10.1111/j.1365-3040.2011.02357.x.

19. Diego, N. D., Sampedro, M. C., Barrio, R. J., Saiz-Fernández, I., Moncaleán, P. et al. (2013). Solute accumulation and elastic modulus changes in six radiata pine breeds exposed to drought. *Tree Physiology, 33,* 69–80. DOI 10.1093/treephys/tps125.

20. Pinheiro, C., António, C., Ortuño, M. F., Dobrev, P. I., Hartung, W. et al. (2011). Initial water deficit effects on lupinus albus photosynthetic performance, carbon metabolism, and hormonal balance: Metabolic reorganization prior to early stress responses. *Journal of Experimental Botany, 62,* 4965–4974. DOI 10.1093/jxb/err194.

21. Miguel, M. D., Guevara, M. N., Sánchez-Gómez, D., María, N. D., Díaz, L. M. et al. (2016). Organ-specific metabolic responses to drought in *Pinus pinaster* Ait. *Plant Physiology and Biochemsity,* 102, 17–26.

22. Dong, Q., Zhang, Z., He, J. X., Zhang, P., Ou, X. B. et al. (2019). Arabidopsis ADF5 promotes stomatal closure by regulating actin cytoskeleton remodeling in response to aba and drought stress. *Journal of Experimental Botany, 70,* 435–446. DOI 10.1093/jxb/ery385.

23. Nurunnaher, A., Islam, M. R., Karim, M. A., Hossain, T. (2014). Alleviation of drought stress in maize by exogenous application of gibberellic acid and cytokinin. *Journal of Crop Science & Biotechnology, 17,* 41–48. DOI 10.1007/s12892-013-0117-3.

24. Remy, E., Cabrito, T. R., Baster, P., Batista, R. A., Teixeira, M. C. et al. (2013). A major facilitator superfamily transporter plays a dual role in polar auxin transport and drought stress tolerance in *Arabidopsis*. *Plant Cell, 25,* 901–926. DOI 10.1105/tpc.113.110353.

25. Shi, J. R., Habben, J. E., Archibald, R. L., Drummond, B. J., Chamberlin, M. A. et al. (2015). Overexpression of argos genes modifies plant sensitivity to ethylene, leading to improved drought tolerance in both *Arabidopsis* and maize. *Plant Physiology, 169,* 266–282. DOI 10.1104/pp.15.00780.

26. Yuan, G. F., Jia, C. G., Li, Z., Sun, B., Zhang, L. P. et al. (2010). Effect of brassinosteroids on drought resistance and abscisic acid concentration in tomato under water stress. *Scientia Horticulturae, 126,* 103–108. DOI 10.1016/j.scienta.2010.06.014.

27. Zhang, L., Li, X., Ma, B., Gao, Q., Du, H. et al. (2017). The tartary buckwheat genome provides insights into rutin biosynthesis and abiotic stress tolerance. *Molecular Plant, 10,* 1224–1237. DOI 10.1016/j.molp.2017.08.013.

28. Zhu, F. (2016). Chemical composition and health effects of tartary buckwheat. *Food Chemistry, 203,* 231–245. DOI 10.1016/j.foodchem.2016.02.050.

29. Bonafaccia, G., Marocchini, M., Kreft, I. (2003). Composition and technological properties of the flour and bran from common and tartary buckwheat. *Food Chemistry, 80,* 9–15. DOI 10.1016/S0308-8146(02)00228-5.

30. Zou, L., Wu, D. T., Ren, G. X., Hu, Y. C., Peng, L. X. et al. (2021). Bioactive compounds, health benefits, and industrial applications of tartary buckwheat (*Fagopdyrum tataricum*). *Critical Reviews in Food Science and Nutrition,* DOI 10.1080/10408398.2021.1952161.

31. Ohnism, O., Tomiyosm, M. (2005). Distribution of cultivated and wild buckwheat species in the NU river valley of Southwestern China. *Fagopyrum, 22,* 1–5.

32. Wan, Y., Ouyang, J. Y., Zhao, G., Xiang, D., Wu, X. et al. (2018). Equipment for Tartary buckwheat during the seed germination. China's Intellectual Property Office, ZL201820533089.1. Beijing, China: China National Intellectual Property Administration.

33. Barrs, H. D., Weatherley, P. E. (1962). A re-examination of the relative turgidity technique for estimating water deficits in leaves. *Australian Journal of Biological Sciences, 115,* 413–428. DOI 10.1071/BI9620413.

34. Blum, A., Ebercon, A. (1981). Cell membrane stability as a measure of drought and heat tolerance in wheat. *Crop Science, 21,* 43–47. DOI 10.2135/cropsci1981.0011183X002100010013x.

35. Hodges, D. M., Delong, J. M., Prange, K. R. K. (1999). Improving the thiobarbituric acid-reactive-substances assay for estimating lipid peroxidation in plant tissues containing anthocyanin and other interfering compounds. *Planta, 207,* 604–611. DOI 10.1007/s004250050524.

36. Giannopolitis, C. N., Ries, S. K. (1977). Superoxide dismutases: I. occurrence in higher plants. *Plant Physiology, 59,* 309–314. DOI 10.1104/pp.59.2.309.

37. Chance, M., Maehly, A. C. (1954). Assay of catalases and peroxidases. *Methods Enzymol, 2,* 764–775. DOI 10.1016/S0076-6879(55)02300-8.

38. Bates, L. S., Waldren, R. P., Teare, I. D. (1973). Rapid determination of free proline for water-stress studies. *Plant Soil, 39,* 205–207. DOI 10.1007/BF00018060.

39. Yemm, E. W., Willis, A. J. (1954). The estimation of carbohydrates in plant extracts by anthrone. *Biochemical. Journal, 57,* 508–514.

40. Peng, B. J., Kuo, M. Y., Yang, P. H., Hewitt, J. T., Boswell, P. G. (2014). A practical methodology to measure unbiased gas chromatographic retention factor *vs.* temperature relationships. *Journal of Chromatography A, 1374,* 207–215. DOI 10.1016/j.chroma.2014.11.018.

41. Okunlola, G. O., Olatunji, O. A., Akinwale, R. O., Tariq, A., Adelusi, A. A. (2017). Physiological response of the three most cultivated pepper species (*Capsicum* spp.) in Africa to drought stress imposed at three stages of growth and development. *Scientia Horticulturae, 224,* 198–205. DOI 10.1016/j.scienta.2017.06.020.

42. Deeba, F., Pandey, A. K., Ranjan, S., Mishra, A., Singh, R. et al. (2012). Physiological and proteomic responses of cotton (*Gossypium herbaceum* L.) to drought stress. *Plant Physiology and Biochemistry, 53,* 6–18. DOI 10.1016/j.plaphy.2012.01.002.

43. Qureshi, M. K., Munir, S., Shahzad, A. N., Rasul, S., Nouman, W. et al. (2018). Role of reactive oxygen species and contribution of new players in defense mechanism under drought stress in rice. *International Journal of Agriculture and Biology, 20,* 1339–1352.

44. Faraji, J., Sepehri, A. (2019). Ameliorative effects of TiO_2 nanoparticles and sodium nitroprusside on seed germination and seedling growth of wheat under peg-stimulated drought stress. *Journal of Seed Science, 41,* 309–317. DOI 10.1590/2317-1545v41n3213139.

45. Gao, S. S., Wang, Y. L., Yu, S., Huang, Y. Q., Liu, H. C. et al. (2020). Effects of drought stress on growth, physiology and secondary metabolites of two adonis species in Northeast China. *Scientia Horticulturae, 259,* 108795DOI 10.1016/j.scienta.2019.108795.

46. Reddy, A. R., Chaitanya, K. V., Vivekanandan, M. (2004). Drought-induced responses of photosynthesis and antioxidant metabolism in higher plants. *Journal of Plant Physiology, 161,* 1189–1202. DOI 10.1016/j.jplph.2004.01.013.

47. Sarker, U., Oba, S. (2018). Catalase, superoxide dismutase and ascorbate-glutathione cycle enzymes confer drought tolerance of amaranthus tricolor. *Scientific Reports, 8,* 16496. DOI 10.1038/s41598-018-34944-0.

48. Cheng, L., Han, M., Yang, L. M., Yang, L., Sun, Z. et al. (2018). Changes in the physiological characteristics and baicalin biosynthesis metabolism of *Scutellaria baicalensis* georgi under drought stress. *Industrial Crops and Products, 122,* 473–482. DOI 10.1016/j.indcrop.2018.06.030.

49. Liu, C. C., Liu, Y. G., Guo, K., Fan, D. Y., Li, G. G. et al. (2011). Effect of drought on pigments, osmotic adjustment and antioxidant enzymes in six woody plant species in karst habitats of Southwestern China. *Environmental and Experimental Botany, 71,* 174–183. DOI 10.1016/j.envexpbot.2010.11.012.

50. Shi, Q., Yin, Y. L., Wang, Z. Q., Fan, W. C., Hua, J. F. (2016). Physiological acclimation of taxodium hybrid 'Zhongshanshan 118' plants to short-term drought stress and recovery. *HortScience, 51,* 1159–1166. DOI 10.21273/HORTSCI10997-16.

51. Szabados, L., Savoure, A. (2010). Proline: A multifunctional amino acid. *Trends Plant Science, 15,* 89–97. DOI 10.1016/j.tplants.2009.11.009.

52. Mansour, M. M. F., Ali, E. (2017). Evaluation of proline functions in saline conditions. *Phytochemistry, 140,* 52–68. DOI 10.1016/j.phytochem.2017.04.016.

53. Cai, J. G., Luo, L. M., Tang, H., Zhou, L. (2018). Cytotoxicity of malondialdehyde and cytoprotective effects of taurine via oxidative stress and PGC-1α signal pathway in C2C12 cells. *Molecular Biology, 52,* 532–542. DOI 10.1134/S0026893318040040.

54. Sadowska-Bartosz, I., Adamczyk, R., Bartosz, G. (2014). Protection against peroxynitrite reactions by flavonoids. *Food Chemistry, 164,* 228–233. DOI 10.1016/j.foodchem.2014.04.105.

55. Jovanovic, S. V., Steenken, S., Hara, Y., Simic, M. G. (1996). Reduction potentials of flavonoid and model phenoxyl radicals. which ring in flavonoids is responsible for antioxidant activity? *Journal of the Chemical Society, Perkin Transactions, 2(11),* 2497–2504. DOI 10.1039/p29960002497.

56. Fini, A., Guidi, L., Ferrini, F., Brunetti, C., Ferdinando, M. et al. (2012). Drought stress has contrasting effects on antioxidant enzymes activity and phenylpropanoid biosynthesis in fraxinus ornus leaves: An excess light stress affair?. *Journal of Plant Physiology, 169,* 929–939. DOI 10.1016/j.jplph.2012.02.014.

57. Gharibi, S., Tabatabaei, B. E. S., Saeidi, G., Talebi, M., Matkowski, A. (2019). The effect of drought stress on polyphenolic compounds and expression of flavonoid biosynthesis related genes in achillea pachycephala rech. *Phytochemistry, 162,* 90–98. DOI 10.1016/j.phytochem.2019.03.004.

58. Yu, Y., Lv, Y., Shi, Y. N., Li, T., Chen, Y. C. et al. (2018). The role of phyto-melatonin and related metabolites in response to stress. *Molecules, 23,* 1887. DOI 10.3390/molecules23081887.

59. Ueno, M., Kihara, J., Arase, S. (2015). Tryptamine and sakuranetin accumulation in sekiguchi lesions associated with the light-enhanced resistance of the lesion mimic mutant of rice to *Magnaporthe Oryzae*. *Journal of General Plant Pathology, 81,* 1–4. DOI 10.1007/s10327-014-0560-0.

60. Marchetti, C. F., Ugena, L., Humplik, J. F., Polak, M., Zeljkovic, S. C. et al. (2019). A novel image-based screening method to study water-deficit response and recovery of barley populations using canopy

dynamics phenotyping and simple metabolite profiling. *Frontiers in Plant Science, 10,* 20. DOI 10.3389/fpls.2019.01252.

61. Sun, C. X., Li, M. Q., Gao, X. X., Liu, L. N., Wu, X. F. et al. (2016). Metabolic response of maize plants to multi-factorial abiotic stresses. *Plant Biology, 18(Suppl 1),* 120–9. DOI 10.1111/plb.12305.

62. Singh, M., Kumar, J., Singh, S., Singh, V. P., Prasad, S. M. (2015). Roles of osmoprotectants in improving salinity and drought tolerance in plants: A review. *Reviews in Environmental Science & Biotechnology, 14,* 407–426. DOI 10.1007/s11157-015-9372-8.

63. Aranda, I., Sanchez-Gomez, D., Cadahia, E., de Simon, B. F. (2018). Ecophysiological and metabolic response patterns to drought under controlled condition in open-pollinated maternal families from a *Fagus* sylvatica lL population. *Environmental and Experimental Botany, 150,* 209–221. DOI 10.1016/j.envexpbot.2018.03.014.